

# Mid-flight Propeller Failure Detection and Control of Propeller-deficient Quadcopter using Reinforcement Learning

Rohitkumar Arasanipalai<sup>†,1</sup>, Aakriti Agrawal<sup>†,1</sup> and Debasish Ghose<sup>2</sup>

**Abstract**—Quadcopters can suffer from loss of propellers in mid-flight, thus requiring a need to have a system that detects single and multiple propeller failures and an adaptive controller that stabilizes the propeller-deficient quadcopter. This paper presents reinforcement learning based controllers for quadcopters with 4, 3, and 2 (opposing) functional propellers. The system is adaptive, unlike traditional control system based controllers. In order to develop an end-to-end system, the paper also proposes a novel neural network based propeller fault detection system to detect propeller loss and switch to the appropriate controller. Our simulation results demonstrate a stable quadcopter with efficient waypoint tracking for all controllers. The detection system is able to detect propeller failure within 2.5 seconds and stabilize for all heights above 3 meters.

**Index Terms**—Reinforcement Learning, Robust/Adaptive Control of Robotic Systems, Autonomous Agents, Quadcopter, Controller, Propeller/Actuator Fault Detection.

## I. INTRODUCTION

Autonomous quadcopter UAVs, operating in harsh weather conditions, or even in benign conditions, often suffer from loss of one or multiple propeller(s) mid-flight [1], [2]. Unless the controller is robust enough to enable flight in propeller-deficient condition, the UAV crashes, causing damage to itself, its payload and the surroundings. Some research has been done in making the UAV fly and come down safely when there is propeller loss [3]. However, a complete end-to-end system that detects the failure, or loss of propeller(s), mid-flight and then takes control of the propeller-deficient UAV to enable waypoint tracking or safe landing is still unaddressed in the literature, and is the main goal of our paper.

A quadcopter is a 4 propeller system whose motor velocities provide various combinations of roll, pitch, and yaw. This imparts 6 degrees of freedom to the quadcopter through which it can carry out waypoint tracking. Traditionally, control systems have been used consisting of two loops in the control model (Figure 1); the outer one focusing on waypoint tracking and inner one focusing on stability. The decision system, proposed in this paper, consists of a reinforcement learning agent for the outer loop waypoint tracking and a PD controller for the inner loop stability. Previous work on propeller loss scenarios [3] have developed

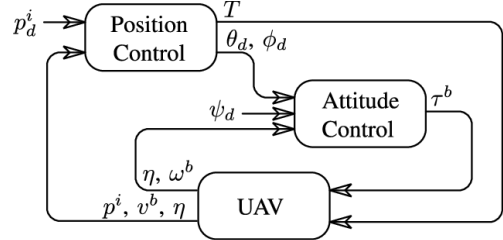


Fig. 1: The inner and outer control loop of a quadcopter [4].

separate control systems for 3, 2 (opposing) and 1 propeller lost system but they did not have an online fault detection (FD) system to switch between the controllers during flight. We propose a novel method using deep learning that detects specific propeller loss using quadcopter state as the input. No additional sensors are used for this purpose, thus avoiding addition of any extra weight to the quadcopter. We then combine it with the different RL agents for the various failed propeller cases (0, 1, and 2 failed propellers). We also show the detection and controller switching when a propeller fails mid-flight. We show that the RL controllers are able to do waypoint tracking even with multiple lost propellers, thus enabling the quadcopter to finish the mission.

The reinforcement learning (RL) setup consists of two major components, an agent and an environment. In our case, the agent is the decision-making system that gives commands to the four motors of the quadcopter (that is, the actions) such that it can autonomously carry out waypoint tracking while being stable in its orientation. The environment is the quadcopter which the agent is acting on. The quadcopter changes its position and orientation when acted upon by the agent. Most RL algorithms follow a similar pattern. First, the environment passes the initial state to the agent, which then acts in order to proceed to the next state. The environment then returns the new state along with the reward of the previous action. Based on the reward, the agents learn which action-state pair maximize the rewards. This loop continues until the terminal state is reached.

**Model-free vs Model-based RL algorithms:** The model based algorithms have complete information about the dynamics of the environment. They learn the transition probability  $T(s_1|(s_0, a))$  from the pair of current state  $s_0$  and action  $a$  to the next state  $s_1$ . Such algorithms are unfeasible in our case due to high dimensional state- and action-space. Therefore, we have used the model-free Proximal Policy Optimization [5] algorithm. This control-agent can also adapt to different conditions if given sufficient time and altitude.

The organization of the paper is as follows: Section

\*Supported by EPSRC Flood Project

<sup>†</sup> Equal Contribution

<sup>1</sup>R. Arasanipalai and A. Agrawal are Research Assistants at Indian Institute of Science, Bangalore, India. e-mail - rohitkumar97@gmail.com and juhi05aakritiagrawal@gmail.com respectively

<sup>2</sup>Debasish Ghose is Professor at Aerospace Department, Indian Institute of Science, Bangalore, India. Email- dghose@iisc.ac.in

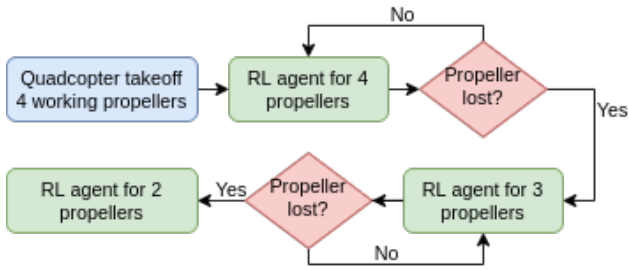


Fig. 2: Flowchart showing the fault detection system along with the RL controllers

II discusses previous related work. Section III describes the proposed decision making system for controlling the quadcopter with failed propellers, Section IV describes the real-time novel fault-detection system for propeller failure and finally Section V integrates these to build an end-to-end system. This is then followed by a thorough comparison of results in Section VI and finally ends with conclusion in Section VII.

## II. RELATED RESEARCH

One of the earliest works that used RL was [6], where model-based RL was used to find an optimal policy for the altitude control loop, yielding a stable controller. Most recent work [7], has used PD controller for stability that is, attitude control loop and an RL agent for waypoint tracking loop. The RL agent learns many different complexities apart from just waypoint tracking, for example, maintaining orientation and stability. Another work [8] has implemented only attitude control using RL, focusing on the inner loop as a first step. These systems adapt to different weather conditions well, but do not address the conditions of propeller-loss.

Fault-tolerant control systems during the loss of only one propeller has been researched extensively [9], [10]. These papers have focused on building angular velocity along the vertical axis and then carry out path following using three propellers. The same idea has been carried forward in recent work by [3], where they have derived the control equation and constraints required to fly a quadcopter with only 3, 2 or 1 functioning propeller. They have shown efficient take-off and waypoint tracking along with stability but have not implemented fault detection required for online switching between different control systems. Similarly, in [11], hover conditions are derived for 3, 2 or 1 propeller lost scenarios. [12] developed combined fault detection and fault-controller system only for loss of a single actuator. Their fault detection strategy is control theory based and have used sliding mode control to combat the actuator loss. The review paper by [13] surveys existing work on fault detection and diagnosis (FDD) and fault-tolerant control (FTC) for unmanned rotorcraft systems from a control theoretic perspective.

The papers [14], [15] monitor the stator current of the motor to relate vibration and current harmonics. Monitoring structural health in real-time on aerospace complex structures has been addressed in [16]. Propeller fault detection with neural networks is done using vibrations produced by the

propeller [17] and by spectral analysis of vibrations from damaged motors [18]. Both of these are offline fault detection systems and serve the purpose of operation check before flight.

In most of the above papers there is no adaptive flight controller with automatic control in case of propeller failure. In contrast to the above papers, we present a learning based combined fault-detection (FD) system for multiple propeller failures and an RL adaptive controller to stabilize the quadcopter post-failure.

## III. CONTROL OF QUADCOPTER WITH 4, 3, AND 2 FUNCTIONAL PROPELLERS USING RL

Three different RL-based controllers for no propeller loss, 1 propeller loss, and 2 propeller loss, are designed. A FD system using recurrent neural networks to identify the propeller(s) that have failed mid-flight, is also implemented. After fault detection, we switch to the appropriate controller mid-flight, thus enabling control and waypoint tracking even after the loss of 1 or 2 propellers. A schematic of our system can be seen in Figure 2.

Out of the two control loops in the quadcopter controller as shown in Figure 1, the inner loop, running at a very high rate, is PD control based. The outer loop, which is for waypoint tracking, has been replaced with RL-based controller.

### A. Quadcopter control using RL

In [7] it was mentioned that out of various policy optimization algorithms like PPO (Proximal Policy Optimization) [5], DGPO (Deep Deterministic Policy Gradient) [19], and TRPO (Trust Region Policy Optimization) [20], PPO gives the best performance on the basis of stability and computation time. Therefore, we have used PPO in a similar implementation. The agent consists of two networks for training, a value network, and a policy network. Both networks have 2 hidden layers of 64 nodes with tanh activation function. The input is the quadcopter state which is an 18-element vector  $q$ :

$$q = [R_{flat}, x, y, z, v_x, v_y, v_z, w_x, w_y, w_z] \quad (1)$$

where,  $R_{flat}$  is the flattened form of quadcopter's rotation matrix,  $(x, y, z)$  is the quadcopter position,  $(v_x, v_y, v_z)$  are the linear, and  $(w_x, w_y, w_z)$  are the angular velocities of the quadcopter. The output is an  $n$ -element vector where  $n$  is the number of functional propellers. We have used Huber loss function [21] for loss calculation of value network and standard gradient descent [22] for policy network.

The exploration strategy for creating the dataset of training consists of three trajectories: initial trajectories, junction trajectories, and branch trajectories. The initial and branch trajectories are on-policy and the junction trajectories are off-policy generated with additive Gaussian noise. The branch trajectories are on-policy trajectories starting from some state along the junction trajectories.

The value function is trained using Monte-Carlo samples that are obtained from the on-policy trajectories. Terminal value, that is, the tail cost of trajectory is taken from the

current value function.

$$v_i = \sum_{t=i}^{T-1} \gamma^{t-i} r_t^p + \gamma^{T-i} V(s_T | \eta) \quad (2)$$

where,  $\eta$  are the parameters of the approximated value function and  $T$  is the length of the trajectory.

**Policy Optimization:** We have used PPO, a policy optimization based algorithm over value iteration based algorithm as given in Algorithm 1.

---

**Algorithm 1** Policy Optimization

---

- 1: Initialize parameters for  $V(s|\eta)$  and  $\pi(s|\theta)$
  - 2: **while**  $j = 1, 2, 3..$  until convergence **do**
  - 3:     Collect data according to **Exploration Strategy**
  - 4:     Compute MC estimate of  $v_i^p$  using Eqn. 2
  - 5:     Update  $V(s|\eta)$   $n_v$  times using Huber loss.
  - 6:     Update  $\pi(s|\theta)$  once using standard gradient descent.
  - 7: **end while**
- 

The quadcopter simulation environment<sup>1</sup> accepts the appropriate action and returns the corresponding rewards and the next state. Multiple environments can be run in parallel which helps in exploration when running the Monte-Carlo simulations.

Our aim is waypoint tracking with a quadcopter without generating a trajectory whenever it is physically possible. During policy optimization, the policy is trained with the origin of the inertial frame as the target waypoint. During operation, the origin of the inertial frame is shifted to the target waypoint. This is done so that the policy need not be explicitly trained on waypoint tracking. The quadcopter is initialized in a random normally distributed state (that is, random position, orientation, angular velocity, and linear velocity) with a reasonable bound such that we can easily explore the feasible state space. Each epoch of the training is done on 500 trajectories, each of which has 500 timesteps.

As mentioned, the quadcopter has a PD controller to maintain stability. The final output is the sum of the output of the two controllers. The PD controller alone is inefficient, but aids in stabilizing the learning process. Without it, the quadcopter simply goes out of bounds due to the random state initialization. The PD controller is given as [7]  $\tau_b = k_p R^T q + k_d R^T w$  where,  $\tau_b$  is the virtual torque produced on the main body as a result of the thrust forces,  $q$  is the orientation matrix,  $R$  is the rotation matrix and  $w$  is the angular velocity. The values of  $k_p$  and  $k_d$  are  $-0.2$  and  $-0.06$ , but for  $z$ -direction it is set to one-sixth of its calculated value. Reward is defined as,

$$r_t = 2 \times 10^{-3} \|p_t\| + 1 \times 10^{-4} \|w_t\| + 5 \times 10^{-4} \|\alpha_t\| \quad (3)$$

<sup>1</sup>The simulation software we have used is the **RAISIM** physics simulator and the **RaisimGym** quadcopter environment (<https://github.com/leggedrobotics/raisimGym>). The interface to this environment is quite similar to the OpenAI gym environment and has a Python interface.

where,  $p_t$  and  $w_t$  are quadcopter's current position and angular velocities, respectively. The angle between quadcopter's vertical axis and  $z$ -axis of the inertial frame is denoted  $\alpha_t$ . Position has a high coefficient since waypoint tracking is the priority of the RL agent. Discount factor value is  $\gamma = 0.99$ .

We have used this same network to train different controllers for no propeller loss, 1 propeller loss, 2 propeller loss with some important modifications for each case. These will be discussed in subsequent sections.

*B. Quadcopter control with no propeller loss*

The RL agent is similar to that defined above. The output of the agent is 4 action values which are motor speeds ( $w = [w_1, w_2, w_3, w_4]$ ). These values are combined with the values from the PD controller to give the final output.

*C. Quadcopter control with one propeller loss*

As derived in [3], for the quadcopter to be in control the controllability matrix shows some constraints. One is that the length of the propellers,  $l \neq 0$ , and the second is  $n_z \neq 0$ , where  $n = (n_x, n_y, n_z)$  is the unit vector governed by the differential equation:  $\dot{n} = -w^B \times n$ . Hence, we conclude that the quadcopter should rotate about a body axis whose vertical component is not 0.

The RL agent gives 3 action outputs ( $w = [w_i, w_{i+1}, w_{i+2}]$ ) which are the motor speeds for the 3 functional motors.

*D. Quadcopter control with two propeller loss*

Similar to the previous section, following [3],  $n_z = 1$  to control the quadcopter with two opposite propellers lost and  $l \neq 0$ . Note that we are not considering the failure of two adjacent propellers, which is an unsolved problem in the literature. The RL agent gives two outputs ( $w = [w_i, w_{i+1}]$ ), which acts on the 2 opposing functional motors.

#### IV. FAULT-DETECTION USING NEURAL NETWORK

Recurrent Neural Networks (RNNs) [23] have been used to exploit the temporal relationship between elements of a sequence by recursively ('unrolling') processing each element. For 1 and 2 lost propellers, the quadcopter exhibits unique set of states at each timestep, which can be classified by an RNN. One problem with RNNs is the exponential growth or decay in the gradient vector for long sequences during training, which prohibits learning long-distance correlations in the sequence. Therefore, we have used LSTM (Long Short Term Memory) [24] which does not have the above issue.

*A. Fault-detection use case*

The task is to map the relationship between the quadcopter states (as defined in Equation 1) and the possible propeller failure states. There are 5 possible states when going from 4 functional propellers to 3 functional propellers: no propeller loss state and each of the 4 propeller loss states. Therefore, the loss state vector  $s \in \mathbb{R}^5$  has elements each denoting probability of belonging to that state.

In case of going from 3 functional propellers to 2 functional (opposing) propellers, we have considered 2 failure states; either the opposite propeller has failed or it has not

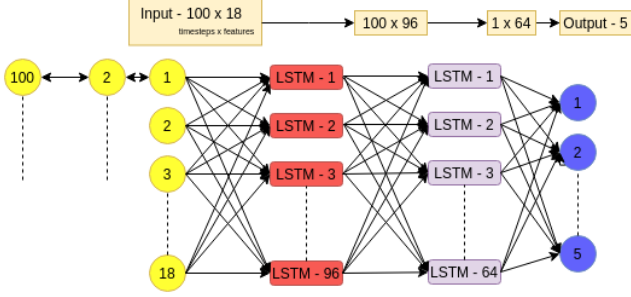


Fig. 3: FD network for  $4 \rightarrow 3$  detection system.

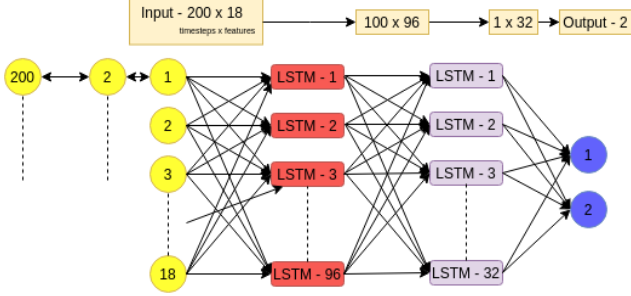


Fig. 4: FD network for  $3 \rightarrow 2$  detection system.

failed. This is because we propose to control quadcopters with only opposite failed propellers. Therefore,  $s \in \mathbb{R}^2$ . Since the elements of  $s$  sum to 1, it means that only one element in  $s$  will have the highest probability. We can now denote the neural network as a function  $f$  trained to map:

$$f : [q_{t-T}, q_{t-T+1}, \dots, q_t] \mapsto s_t \quad (4)$$

where,  $T$  is the window length and  $t$  is the current trajectory timestep.

### B. Network Architecture

For the remainder of this paper, the nomenclature of  $m \rightarrow n$  is used to denote failure cases, where  $m$  is the number of functional propellers before fault occurs, and  $n$ , the number of functional propellers after the fault. For example,  $4 \rightarrow 3$  denotes the quadcopter going from 4 functional propellers to 3 functional propellers after a propeller failure.

1)  $4 \rightarrow 3$  fault-detection (FD) network: It consists of 96 LSTM cells in the first layer and 64 LSTM cells in the second layer (See Figure 3). The second layer passes into the output feedforward layer which has 5 nodes for the 5 possible classes/states. The optimizer used is Stochastic Gradient Descent (SGD) [22] with momentum. Momentum allows the network to converge over a wide range of learning rates [25] thus allowing us to prototype multiple networks quickly.

2)  $3 \rightarrow 2$  fault-detection (FD) network: It consists of 96 LSTM cells in the first layer and 32 LSTM cells in the second layer (See Figure 4). It then passes through feedforward layer with 2 nodes for the 2 possible classes. The optimizer used is Adam [26].

The **training parameters** are listed in the table I. We chose a *computationally cheap network* with only two LSTM

layers for two reasons. Firstly, the network needs to run on the drone in real-time. Drones generally have a light CPU and GPU. Secondly, even small networks can learn very complex contextual information. Our network gave highly accurate results and thus there was no need for a complicated network.

	$4 \rightarrow 3$ Transition Network	$3 \rightarrow 2$ Transition Network
Optimizer	Stochastic Gradient Descent	Adam
Learning Rate	$10^{-4}$	$10^{-4}$
Momentum	0.9	-
No. of Training Epochs	95	416
Final Training Accuracy	97%	92%

TABLE I: Training parameters for the 2 networks

We have used a window size ( $T$ ) of 100 for  $4 \rightarrow 3$  FD network and 200 for  $3 \rightarrow 2$  FD network as shown in Figure 3 and 4, respectively. Using a lower window size of 50 and 100 for the two networks, respectively, gave lower accuracy in the predictions because we needed more timesteps to establish the relationship between quadcopter behavior and propeller loss. Larger window length is likely to increase the fault-detection time as well which is undesirable.

The first 150 timesteps for the  $4 \rightarrow 3$  FD network and 250 timesteps for the  $3 \rightarrow 2$  FD network are skipped. This is because the quadcopter is initialized in a random state and we do not want the network to learn this initial erratic behaviour that occurs until stabilization. Instead, we want the network to learn the erratic behaviour when a propeller loss occurs. Thus, the RNN does not need to learn to differentiate between the two behaviors, as the initial erratic behavior is unlikely to be encountered in actual scenarios.

Let the  $4 \rightarrow 3$  FD network, with a window of 100 and starting from 151<sup>st</sup> sample be represented as function  $f_{4 \rightarrow 3}$ . Following equation 4 the input and output can be related as,

$$f_{4 \rightarrow 3}(q_{t-100}, q_{t-99}, \dots, q_t) = s_t, \text{ where } t > 150 \quad (5)$$

Similarly, for the  $3 \rightarrow 2$  FD network, with a window of 200 and starting from 251<sup>st</sup> sample are related as,

$$f_{3 \rightarrow 2}(q_{t-200}, q_{t-199}, \dots, q_t) = s_t, \text{ where } t > 250 \quad (6)$$

## V. COMPLETE SYSTEM

The complete end-to-end system is shown in Algorithm 2. We assume that the quadcopter starts with 4 working propellers. The RL agent based controller for 4 propeller is engaged. The  $4 \rightarrow 3$  FD network continuously checks for propeller failure at every loop. There are four cases here for each of the four propellers of the quadcopter, that is, either propeller 1 fails or propeller 2 fails and so on. Once a propeller failure is detected, the same is updated and the controller for 3 propellers is engaged. From this point onward, the  $3 \rightarrow 2$  FD network takes over and checks for the second propeller loss. Similar to above, if it encounters 2<sup>nd</sup> (opposing) propeller failure, it switches to 2 propeller controller.

### A. Removing offset

Deep reinforcement learning suffers from the bias vs variance paradigm. PPO algorithm has less variance and therefore can learn complex policies. But it suffers from the

---

**Algorithm 2** Fault detection and control in quadcopter
 

---

```

1: Initialize quadcopter
2: Initialize prop_lost  $\leftarrow 0$ 
3: Take-off quadcopter
4: Initialize 4  $\rightarrow$  3 and 3  $\rightarrow$  2 fault-detection network with
   trained weights
5: while  $t = 1, 2, 3, \dots$  until quadcopter lands do
6:   if prop_lost == 0 then
7:     action  $\leftarrow$  4_propeller_controller; 4  $\rightarrow$  3 FD
       network
8:     if 4  $\rightarrow$  3 FD network == True then
9:       prop_lost  $\leftarrow 1$ 
10:    end if
11:   else if prop_lost == 1 then
12:     action  $\leftarrow$  3_propeller_controller; 3  $\rightarrow$  2 FD
       network
13:     if 3  $\rightarrow$  2 FD network == True then
14:       prop_lost  $\leftarrow 2$ 
15:     end if
16:   else
17:     action  $\leftarrow$  2_propeller_controller
18:   end if
19: end while
  
```

---

problem of bias and produces a small, but constant offset between the quadcopter's position and the required position. In order to account for this offset we use a moving average filter with a window of 15 time-steps, and average the quadcopter's actual position within this window. Since our required position is the origin of the inertial frame  $([0, 0, 0])$  and our model is trained for that position, we add the moving average value to the quadcopter's actual position.

Let the quadcopter's actual position at the  $t^{th}$  time instant be  $x(t), y(t), z(t)$  and  $\bar{x}(t), \bar{y}(t), \bar{z}(t)$  be the moving average in  $x, y$ , and  $z$  direction. Therefore,

$$\bar{p}(t) = \frac{\sum_{i=t-15}^{t+15} p_{i-15}}{15} \text{ where, } p = x, y, z. \quad (7)$$

Now add  $\bar{p}$  offset to the quadcopter's actual position, to make it the quadcopter's observed position.

## VI. RESULT

We have evaluated the performance of the 3 controllers individually, as well as in combination, while the quadcopter is performing waypoint tracking. We have plotted its position  $(x, y, z)$  and angular velocity  $(w_x, w_y, w_z)$  to demonstrate waypoint tracking and stability. The quadcopter is initialized at the origin and is directed to reach height ( $z$ ) of 5m, simulating a take off. After 10 seconds, the target-waypoint is shifted by 1m in the positive Y direction. In the propeller loss scenarios, the propeller is turned off manually and time taken to regain stability is calculated.

### A. Implementation for no propeller loss

As can be seen from figure 5, the policy is able to track the waypoint accurately while keeping the quadcopter stable

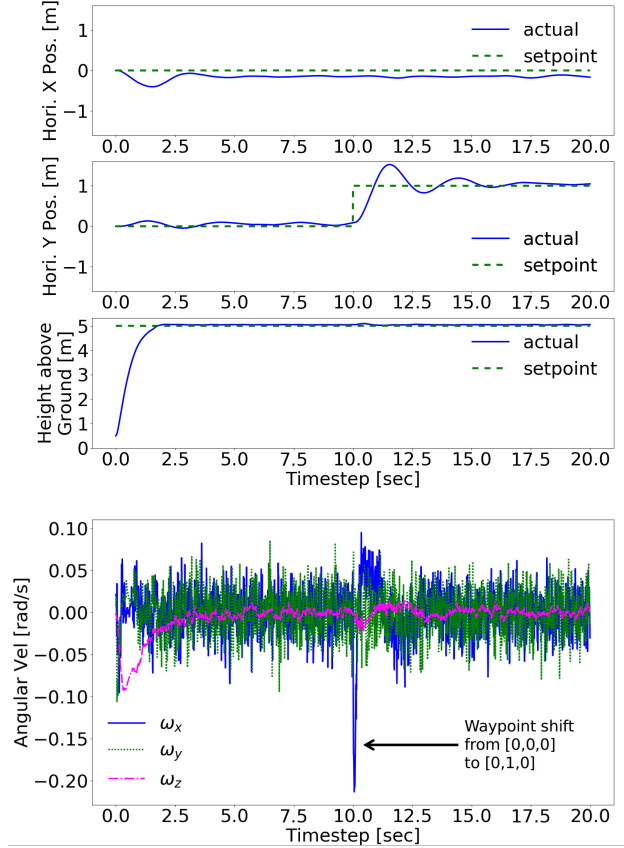


Fig. 5: Quadcopter with no propeller loss.

with near 0 angular velocities. It is also able to accommodate the waypoint shift to  $[0, 1, 5]$ . These results are comparable with [7] on which our RL agent is based. Thus, this RL agent can be used to replace the LQR controller [27] for a healthy quadcopter.

### B. Implementation for one propeller loss

As shown in [3], on losing a single propeller, the quadcopter loses one degree of freedom and to maintain stability, a non-zero angular velocity about the vertical axis has to be enforced. Figure 6 shows the position and angular velocity of the quadcopter when it takes off with a single broken propeller. As can be seen from the graphs, the quadcopter has a constant yaw rate of approximately 1.0 rad/s. The graphs also demonstrate that even after losing a propeller, the quadcopter is able to track the waypoint shift occurring at 10 seconds into the simulation. There is a constant offset in position which is solved as described in subsection V-A. On comparing these results with [3] (where the value is  $19 \text{ rad s}^{-1}$ , which could be due to the assumed dynamical model), we get comparable results in position and angular velocity. Thus, our RL agent can replace the traditional model-based control system.

### C. Implementation for two propeller loss

Figure 7 shows similar results for the loss of two propellers on a quadcopter system. There is a constant yaw rate of

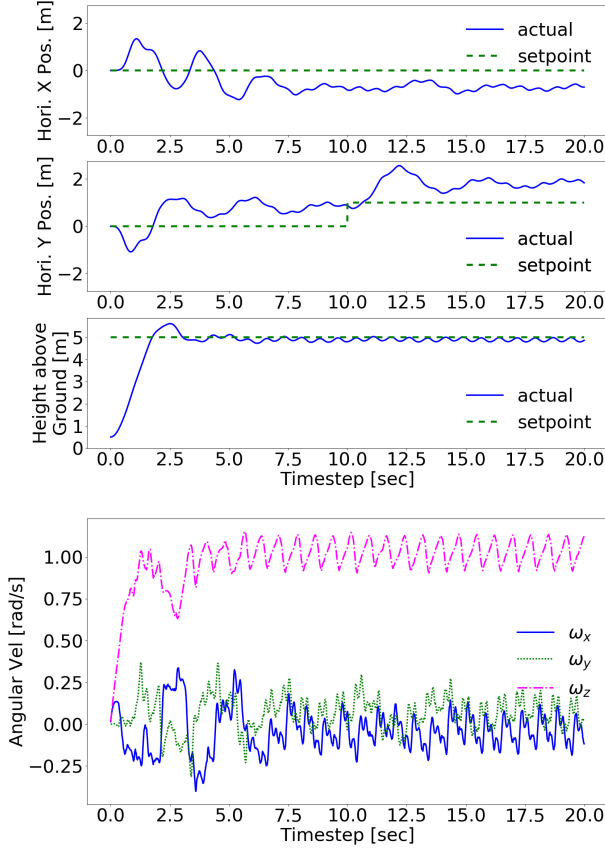


Fig. 6: One propeller lost.

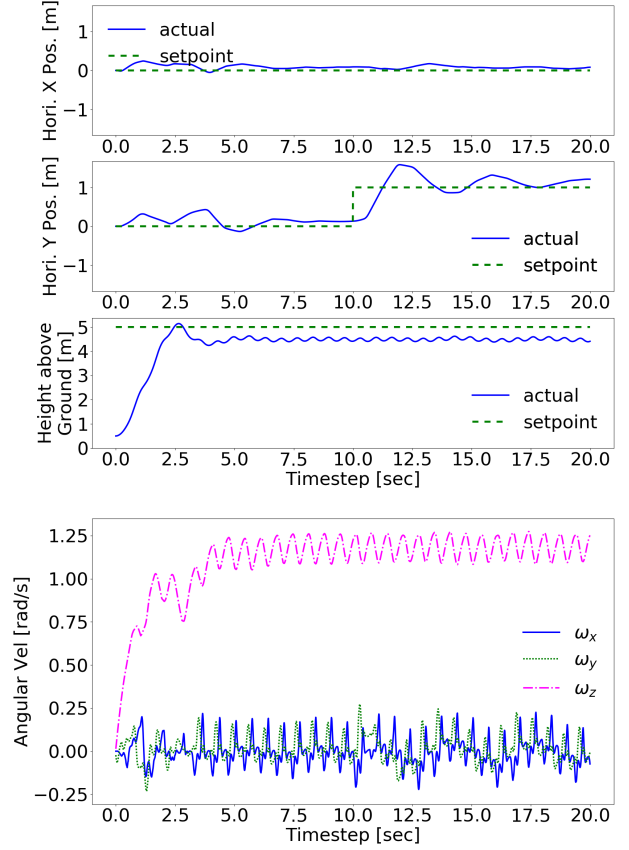


Fig. 7: Two propellers lost.

around  $1.2 \text{ rad s}^{-1}$ , which is quite close to the yaw rate of one propeller-lost system. This angular velocity is lower compared to the results of [3] (where the value is  $30.1 \text{ rad s}^{-1}$ , again, which could be due to the assumed dynamical model), thus showing that this RL agent is able to produce more stable results. The offset in position is larger compared to the single propeller-lost case, but can be solved using the method described in subsection V-A. The graphs demonstrate that the quadcopter is stable and is able to carry out waypoint tracking as evidenced by it accommodating the waypoint shift. We can, therefore, adjust the target waypoints in a similar manner to perform soft landing in real-life situations.

#### D. Integrating fault detection with the control agents

1) *Transition from 4 working propellers to 3 working propellers:* Figure 8 shows the behavior of the quadcopter when a propeller fails mid-flight. The FD system identifies the failed propeller and switches to the appropriate control agent. The 2 vertical lines in the graphs represents the actual time at which the propeller failed and time at which the fault was detected, respectively. The graph shows a 1 second delay between the failure and its detection. Table II shows the average time of detection for 5 runs with failure occurring at random timesteps.

2) *Transition from 3 working propellers to 2 working propellers:* Figure 9 shows the behavior of the quadcopter when the second propeller also fails mid-flight. The  $3 \rightarrow 2$

Propellers Lost	1st	2nd
Time (secs)	0.92	2.25

TABLE II: The average time taken to detect first and second propeller loss

FD system kicks in and identifies the failed propeller and switches to the appropriate control agent. The 2 vertical lines in the graphs represents the actual time at which the propeller failed and the time at which the fault was detected, respectively. As can be seen, there is a delay of around 2.24 seconds between the propeller failure and its detection. From table II, we can also see the average time of detection for 5 runs, in which the failure occurs at random timesteps.

#### E. Failure rate calculation

In this paper, the failure condition for the quadcopter is whenever it touches the ground. The failure rate is recorded from 500 runs with random initialization of orientation, position, linear and angular velocity. The orientation was

	Failure Rate (%)
Control agent - No propeller loss	2
Control agent - One propeller loss	16.4
Control agent - Two propeller loss	32

TABLE III: The failure rate (in 500 runs) for independent control agents and various propeller loss cases.

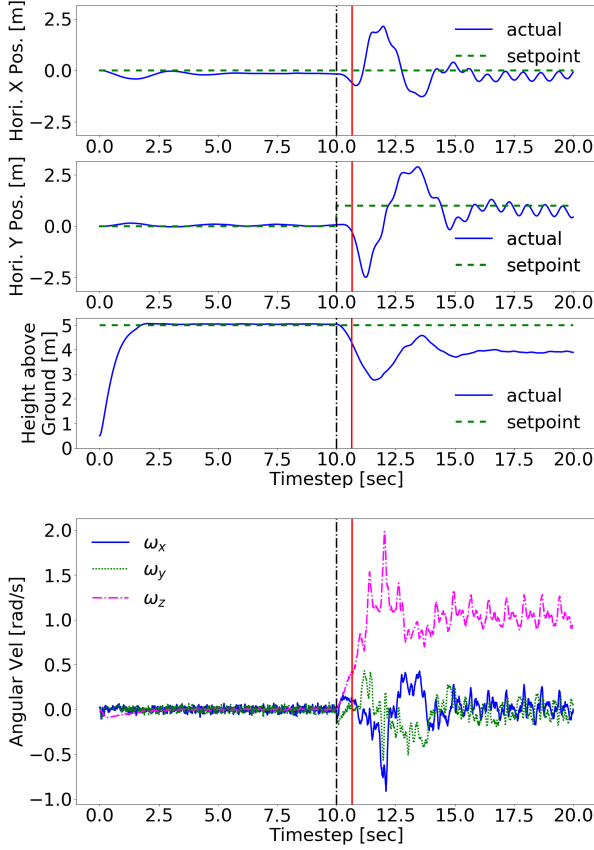


Fig. 8: Sudden propeller lost in mid-flight.

sampled uniformly in  $SO(3)$  and the other quantities were sampled uniformly in  $[-1, 1]$ . For the 4, 3, and 2 propeller scenarios, the target height was fixed at 5 meters above the ground. The results are tabulated in Table III. The random initialization in the isolated 4, 3, and 2 propeller scenarios caused some quadcopters to start in an irrecoverable state, for example, upside down or very high linear velocity towards the ground and so on. Recovery from some states, in case of 1 or 2 propeller loss, becomes harder due to the lost degree-of-freedom and insufficient thrust, thus increasing the failure rate.

Figure 10 shows the failure rate when propellers are lost mid flight from both  $4 \rightarrow 3$  and  $3 \rightarrow 2$  cases. The target height of the quadcopter in the 500 runs was evenly distributed between 2m-3m from  $4 \rightarrow 3$  and 0.5m-1.5m for  $3 \rightarrow 2$  scenarios. From the figures, we are able to find a height threshold at which the failure recovery system is not able to switch in time and stop the quadcopter from crashing to the ground. Videos showing the experiments in detail can be found [here](#)<sup>2</sup> and implementation code [here](#)<sup>3</sup>.

## VII. CONCLUSIONS

In this paper, we have proposed a system for mid-flight failure detection and control in case of multiple propeller

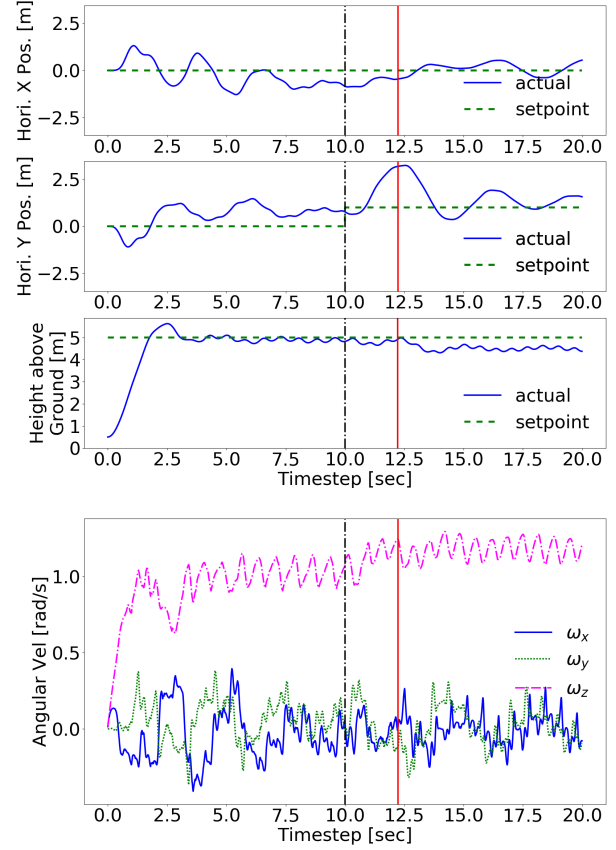


Fig. 9: Three propeller quadcopter with second propeller (opposing) lost in mid-flight.

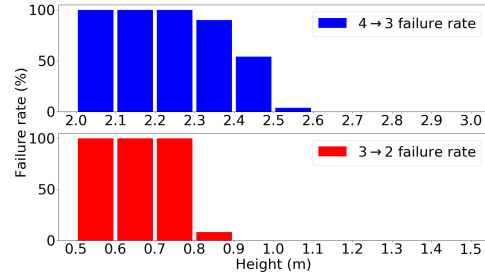


Fig. 10: Failure rate of  $4 \rightarrow 3$  and  $3 \rightarrow 2$  in 500 runs spread across a height range of 1 meter.

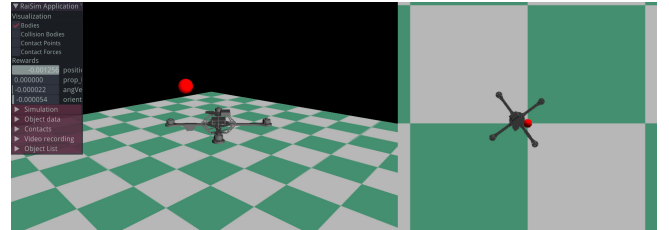


Fig. 11: Still image from the simulation showing the quadcopter and the target waypoint (red dot).

loss in a quadcopter. Firstly, we showed how RL agents can learn to control quadcopters with 0, 1 and 2 (opposing) propeller(s) lost. We showed that the quadcopter learned to

<sup>2</sup><https://youtu.be/SexeCnUizY>

<sup>3</sup><https://github.com/Aakriti05/Prop-Fail-Detect-Control-RL>

do waypoint tracking while maintaining stability, even with 1 and 2 (opposing) propeller(s) failed. Secondly, we developed a novel fault detection system using deep learning which can detect the propeller(s) failure and switch to the appropriate controller. This method requires only the previous states of the quadcopter and is able to detect the propeller loss within 2.5 seconds, thus removing the need and maintenance for any additional sensor hardware on the quadcopter. We have also shown, in simulation, that the detection and switching can happen in real-time, preventing the quadcopter from crashing and enabling it to either land or continue its mission.

Future scope of this work can be to replace the inner loop based on PD controller, with an RL agent to make the whole system model-free, and completely discard the need to develop a mathematical model of the quadcopter. The real-time implementation of this system is also the next step of this research work. One can also implement a health monitoring system to check if the non-functional propeller becomes functional again, enabling switch to the appropriate controller.

## REFERENCES

- [1] A. Birk, B. Wiggerich, H. Bülow, M. Pfingsthorn, and S. Schwertfeger, "Safety, security, and rescue missions with an unmanned aerial vehicle (UAV)," *Journal of Intelligent & Robotic Systems*, vol. 64, no. 1, pp. 57–76, Oct 2011.
- [2] D. Erdos, A. Erdos, and S. E. Watkins, "An experimental UAV system for search and rescue challenge," *IEEE Aerospace and Electronic Systems Magazine*, vol. 28, no. 5, pp. 32–37, May 2013.
- [3] M. W. Mueller and R. D'Andrea, "Stability and control of a quadcopter despite the complete loss of one, two, or three propellers," in *2014 IEEE International Conference on Robotics and Automation (ICRA)*, May 2014, pp. 45–52.
- [4] N. Cao and A. F. Lynch, "Innerouter loop control for quadrotor uavs with input and state constraints," *IEEE Transactions on Control Systems Technology*, vol. 24, no. 5, pp. 1797–1804, Sept 2016.
- [5] J. Schulman, F. Wolski, P. Dhariwal, A. Radford, and O. Klimov, "Proximal policy optimization algorithms," *arXiv:1707.06347 [cs.LG]*, Aug 2017.
- [6] S. L. Waslander, G. M. Hoffmann, Jung Soon Jang, and C. J. Tomlin, "Multi-agent quadrotor testbed control design: integral sliding mode vs. reinforcement learning," in *IEEE/RSJ International Conference on Intelligent Robots and Systems*, Aug 2005, pp. 3712–3717.
- [7] J. Hwangbo, I. Sa, R. Siegwart, and M. Hutter, "Control of a quadrotor with reinforcement learning," *IEEE Robotics and Automation Letters*, vol. 2, no. 4, pp. 2096–2103, Oct 2017.
- [8] W. Koch, R. Mancuso, R. West, and A. Bestavros, "Reinforcement learning for UAV attitude control," *ACM Transactions on Cyber-Physical System*, vol. 3, no. 2, pp. 22:1–22:21, Feb. 2019.
- [9] A. Akhtar, S. L. Waslander, and C. Nielsen, "Fault tolerant path following for a quadrotor," in *52nd IEEE Conference on Decision and Control*, Dec 2013, pp. 847–852.
- [10] A. Freddi, A. Lanzon, and S. Longhi, "A feedback linearization approach to fault tolerance in quadrotor vehicles," *IFAC Proceedings Volumes*, vol. 44, no. 1, pp. 5413 – 5418, 2011.
- [11] M. W. Mueller and R. D'Andrea, "Relaxed hover solutions for multi-copters: Application to algorithmic redundancy and novel vehicles," *The International Journal of Robotics Research*, vol. 35, no. 8, pp. 873–889, 2016.
- [12] N. Nguyen and S. Hong, "Fault diagnosis and fault-tolerant control scheme for quadcopter UAVs with a total loss of actuator," *Energies*, vol. 12, p. 1139, Mar 2019.
- [13] Y. Zhang, A. Chamseddine, C. Rabbath, B. Gordon, C.-Y. Su, S. Rakheja, C. Fulford, J. Apkarian, and P. Gosselin, "Development of advanced FDD and FTC techniques with application to an unmanned quadrotor helicopter testbed," *Journal of the Franklin Institute*, vol. 350, no. 9, pp. 2396 – 2422, 2013.
- [14] C. M. Riley, B. K. Lin, T. G. Habetler, and R. R. Schoen, "A method for sensorless on-line vibration monitoring of induction machines," *IEEE Transactions on Industry Applications*, vol. 34, no. 6, pp. 1240–1245, Nov 1998.
- [15] R. R. Schoen, T. G. Habetler, F. Kamran, and R. G. Bartfield, "Motor bearing damage detection using stator current monitoring," *IEEE Transactions on Industry Applications*, vol. 31, no. 6, pp. 1274–1279, Nov 1995.
- [16] Y. K. Yap, "Structural health monitoring for unmanned aerial systems," Master's thesis, EECS Department, University of California, Berkeley, May 2014.
- [17] G. Iannace, G. Ciaburro, and A. Trematerra, "Fault diagnosis for UAV blades using artificial neural network," *Robotics*, vol. 8, p. 59, Jul 2019.
- [18] B. Ghalamchi and M. Mueller, "Vibration-based propeller fault diagnosis for multicopters," in *2018 International Conference on Unmanned Aircraft Systems (ICUAS)*, June 2018, pp. 1041–1047.
- [19] T. P. Lillicrap, J. J. Hunt, A. Pritzel, N. M. O. Heess, T. Erez, Y. Tassa, D. Silver, and D. Wierstra, "Continuous control with deep reinforcement learning," *arXiv:1509.02971 [cs.LG]*, Sept 2015.
- [20] J. Schulman, S. Levine, P. Abbeel, M. Jordan, and P. Moritz, "Trust region policy optimization," in *International Conference on Machine Learning, ICML*, vol. 37, July 2015, pp. 1889–1897.
- [21] P. J. Huber, "Robust estimation of a location parameter," *The Annals of Mathematical Statistics*, vol. 35, no. 1, pp. 73–101, Mar 1964.
- [22] J. Kiefer and J. Wolfowitz, "Stochastic estimation of the maximum of a regression function," *Ann. Math. Statist.*, vol. 23, no. 3, pp. 462–466, Sept 1952.
- [23] J. L. Elman, "Finding structure in time," *Cognitive Science*, vol. 14, no. 2, pp. 179 – 211, 1990.
- [24] S. Hochreiter and J. Schmidhuber, "Long short-term memory," *Neural Comput.*, vol. 9, no. 8, pp. 1735–1780, Nov. 1997.
- [25] N. Qian, "On the momentum term in gradient descent learning algorithms," *Neural Networks*, vol. 12, no. 1, pp. 145 – 151, 1999.
- [26] D. P. Kingma and J. Ba, "Adam: A method for stochastic optimization," in *International Conference on Learning Representations (ICLR)*, Dec 2015.
- [27] D. P. Bertsekas, *Dynamic Programming and Optimal Control*, 2nd ed. Athena Scientific, 2000.